

# **SANDIA REPORT**

SAND2009-6091

Unlimited Release

Printed September 2009

## **A Fully Implicit Method for 3D Quasi-Steady State Magnetic Advection-Diffusion**

Christopher M. Siefert  
Allen C. Robinson

Prepared by  
Sandia National Laboratories  
Albuquerque, New Mexico 87185 and Livermore, California 94550

Sandia is a multiprogram laboratory operated by Sandia Corporation,  
a Lockheed Martin Company, for the United States Department of Energy's  
National Nuclear Security Administration under Contract DE-AC04-94-AL85000.

Approved for public release; further dissemination unlimited.



**Sandia National Laboratories**

Issued by Sandia National Laboratories, operated for the United States Department of Energy by Sandia Corporation.

**NOTICE:** This report was prepared as an account of work sponsored by an agency of the United States Government. Neither the United States Government, nor any agency thereof, nor any of their employees, nor any of their contractors, subcontractors, or their employees, make any warranty, express or implied, or assume any legal liability or responsibility for the accuracy, completeness, or usefulness of any information, apparatus, product, or process disclosed, or represent that its use would not infringe privately owned rights. Reference herein to any specific commercial product, process, or service by trade name, trademark, manufacturer, or otherwise, does not necessarily constitute or imply its endorsement, recommendation, or favoring by the United States Government, any agency thereof, or any of their contractors or subcontractors. The views and opinions expressed herein do not necessarily state or reflect those of the United States Government, any agency thereof, or any of their contractors.

Printed in the United States of America. This report has been reproduced directly from the best available copy.

Available to DOE and DOE contractors from  
U.S. Department of Energy  
Office of Scientific and Technical Information  
P.O. Box 62  
Oak Ridge, TN 37831

Telephone: (865) 576-8401  
Facsimile: (865) 576-5728  
E-Mail: [reports@adonis.osti.gov](mailto:reports@adonis.osti.gov)  
Online ordering: <http://www.doe.gov/bridge>

Available to the public from  
U.S. Department of Commerce  
National Technical Information Service  
5285 Port Royal Rd  
Springfield, VA 22161

Telephone: (800) 553-6847  
Facsimile: (703) 605-6900  
E-Mail: [orders@ntis.fedworld.gov](mailto:orders@ntis.fedworld.gov)  
Online ordering: <http://www.ntis.gov/help/ordermethods.asp?loc=7-4-0#online>



SAND2009-6091  
Unlimited Release  
Printed September 2009

# A Fully Implicit Method for 3D Quasi-Steady State Magnetic Advection-Diffusion

Christopher M. Siefert  
Allen C. Robinson  
Computational Shock and Multiphysics

Sandia National Laboratories  
P.O. Box 5800  
Albuquerque, NM 87185-0819

## Abstract

We describe the implementation of a prototype fully implicit method for solving three-dimensional quasi-steady state magnetic advection-diffusion problems. This method allows us to solve the magnetic advection diffusion equations in an Eulerian frame with a fixed, user-prescribed velocity field. We have verified the correctness of method and implementation on two standard verification problems, the Solberg-White magnetic shear problem and the Perry-Jones-White rotating cylinder problem.

This page intentionally left blank.

# Contents

<b>Nomenclature</b>	<b>8</b>
<b>1 Introduction</b>	<b>9</b>
<b>2 Theory</b>	<b>9</b>
<b>3 Verification Experiments</b>	<b>11</b>
3.1 Solberg-White MHD Shear Problem . . . . .	12
3.2 Perry-Jones-White Rotating Cylinder Problem . . . . .	13
<b>4 Conclusions</b>	<b>16</b>
<b>References</b>	<b>18</b>
<b>A Detailed Verification Results</b>	<b>19</b>
A.1 Solberg-White MHD Shear Problem . . . . .	19
A.2 Perry-Jones-White Rotating Cylinder Problem . . . . .	19

## List of Figures

1	Order verification for Solberg-White MHD shear problem . . . . .	12
2	Perry-Jones-White steady-state $\mathbf{B}_x$ and $\mathbf{B}_y$ . . . . .	15
3	Order verification ( $\mathbf{B}_x$ ) for Perry-Jones-White rotating cylinder . . . . .	16
4	Order verification ( $\mathbf{B}_y$ ) for Perry-Jones-White rotating cylinder . . . . .	17

## List of Tables

1	CPU time for Solberg-White MHD shear problem . . . . .	13
2	CPU time for Perry-Jones-White rotating cylinder . . . . .	14
3	MHD order verification for Solberg-White MHD shear problem . . . . .	19
4	QSM order verification for Solberg-White MHD shear problem . . . . .	19
5	$\mathbf{B}_x$ QSM order verification for Perry-Jone-White rotating cylinder . . . . .	20
6	$\mathbf{B}_y$ QSM order verification for Perry-Jone-White rotating cylinder . . . . .	20

# Nomenclature

$\sigma(x)$	user specified spatial conductive function
$\mathbf{v}(x)$	user specified spatial velocity function satisfying $\nabla \cdot \mathbf{v} = 0$

# 1 Introduction

This report documents the implementation and testing of a fully implicit method for solving the three dimensional quasi-steady state magnetic advection-diffusion equations. These equations remain from the full magnetohydrodynamics model when the velocity field is assumed to be known. This approach avoids the limitations associated with explicitly capturing acoustic waves and can proceed integrate in time to steady state using very large timesteps. In order to assure highly accurate solutions, we have employed curl-compatible discretizations, also known as edge elements [2, 3]. Our existing scalable linear solver technology [1] has been employed to solve the resulting discrete system. This approach provides for highly efficient "mid-level" modeling when the kinematics of the flow field can be assumed.

In the end we are interested in solving the advection diffusion equation in regimes in which the magnetic Reynold's number,

$$R_M = \mu\sigma|\mathbf{v}|L, \quad (1.1)$$

varies by orders of magnitude from very small to very large values. The number provides a measure of the relative strength of the advective versus diffusive terms in this moving conducting media model. At very small values the solution will be dominated by diffusion while for very large magnetic values,  $R_M \gg 1$ , the convective effects on the magnetic field due to material motion will be balanced where required by very small length scale diffusion layers. We expect in this case that the equations will need to be stabilized when the resolution of the simulation is not such that that small diffusion layers are adequately resolved. Such stabilization is not discussed in this report.

We have verified the correctness of our method on two standard verification problems, the Solberg-White magnetic shear problem and the Perry-Jones-White rotating cylinder problem. For both of these problems, we compare our quasi-steady state method with the appropriate analytic solution. For the Solberg-White problem, where we have an orthogonal mesh and a smoothly varying velocity field, we demonstrate that our quasi-steady method converges at second order accuracy with respect to spatial refinement. For the Perry-Jones-White problem, which has a discontinuous velocity field and somewhat distorted elements, we demonstrate first order convergence in space.

## 2 Theory

The basic approximate model equation that we consider is Faraday's induction equation in moving media. In integral form this is

$$\frac{d}{dt} \int_{\Gamma_t} \mathbf{B} \cdot \mathbf{n} \, d\Gamma + \oint_{\partial\Gamma_t} \mathcal{E} \cdot d\mathbf{x} = 0, \quad (2.2)$$

where  $\partial\Gamma_t$  is the boundary of the material surface  $\Gamma_t$ ,  $\mathbf{B}$  is the magnetic induction or magnetic flux density and  $\mathcal{E}$  is the electromotive intensity or the electric field in the material frame. In local form this is

$$\frac{\partial\mathbf{B}}{\partial t} - \nabla \times (\mathbf{v} \times \mathbf{B}) + (\nabla \cdot \mathbf{B})\mathbf{v} + \nabla \times \mathcal{E} = 0, \quad (2.3)$$

where  $\mathbf{v}$  is the velocity field. The magnetic induction is divergence free, namely,

$$\nabla \cdot \mathbf{B} = 0. \quad (2.4)$$

Ampere's Law neglecting displacement currents

$$\nabla \times \mathbf{H} = \mathbf{J}, \quad (2.5)$$

relates the magnetic field  $\mathbf{H}$  and the current density  $\mathbf{J}$ . We also have Ohm's Law

$$\mathbf{J} = \sigma\mathcal{E}, \quad (2.6)$$

relating the current density to the electromotive intensity and

$$\mathbf{H} = \frac{\mathbf{B}}{\mu}, \quad (2.7)$$

relating the magnetic field and the flux density. We can chose to include an arbitrary scalar potential  $\phi$  in the formulation. In this case we need one additional equation or "gauge" to close the system. A useful choice is

$$\nabla \cdot \sigma\nabla\phi = 0. \quad (2.8)$$

This clearly separates steady state potential electric field solution contributions from the transient solution. We can relate the electromotive intensity to the electric field in the lab frame,  $\mathbf{E}$ , by

$$\mathcal{E} = \mathbf{E} + \mathbf{v} \times \mathbf{B} - \nabla\phi. \quad (2.9)$$

Combining these equations results in

$$\nabla \times \frac{\mathbf{B}}{\mu} = \sigma\mathcal{E}, \quad (2.10)$$

$$\frac{\partial\mathbf{B}}{\partial t} + \nabla \times \mathbf{E} = 0, \quad (2.11)$$

$$\mathcal{E} = \mathbf{E} + \mathbf{v} \times \mathbf{B} - \nabla\phi. \quad (2.12)$$

We weakly impose Ampere's law and directly discretize Faraday's law. Our finite element representation is

$$\int_{\Omega} \frac{\mathbf{B}}{\mu} \cdot \nabla \times \hat{\mathbf{E}} d\Omega + \int_{\Gamma} (\mathbf{n} \times \mathbf{H}_b) \cdot \hat{\mathbf{E}} d\Gamma = \int_{\Omega} \sigma\mathcal{E} \cdot \hat{\mathbf{E}} d\Omega, \quad (2.13)$$

$$\frac{\mathbf{B}^{n+1} - \mathbf{B}^n}{\Delta t} + \nabla \times \mathbf{E} = 0, \quad (2.14)$$

$$\int_{\Omega} \nabla\hat{\phi} \cdot \sigma\nabla\phi d\Omega = \int_{\Gamma} \hat{\phi}\sigma\nabla\phi \cdot \mathbf{n} d\Gamma. \quad (2.15)$$

Substituting (2.12) and (2.14) into (2.13) yields

$$\int_{\Omega} \mu^{-1} (\mathbf{B}^n - \Delta t \nabla \times \mathbf{E}) \cdot \nabla \times \hat{\mathbf{E}} \, d\Omega + \int_{\Gamma} (\mathbf{n} \times \mathbf{H}_b) \cdot \hat{\mathbf{E}} \, d\Gamma = \int_{\Omega} \sigma (\mathbf{E} + \mathbf{v} \times (\mathbf{B}^n - \Delta t \nabla \times \mathbf{E}) - \nabla \phi) \cdot \hat{\mathbf{E}} \, d\Omega, \quad (2.16)$$

or,

$$\int_{\Omega} \sigma \mathbf{E} \cdot \hat{\mathbf{E}} + \frac{\Delta t}{\mu} (\nabla \times \mathbf{E}) \cdot (\nabla \times \hat{\mathbf{E}}) - \sigma \Delta t \mathbf{v} \times (\nabla \times \mathbf{E}) \cdot \hat{\mathbf{E}} \, d\Omega = \int_{\Omega} \frac{1}{\mu} \mathbf{B}^n \cdot \nabla \times \hat{\mathbf{E}} - \sigma (\mathbf{v} \times \mathbf{B}^n) \cdot \hat{\mathbf{E}} + \sigma \nabla \phi \cdot \hat{\mathbf{E}} \, d\Omega + \int_{\Gamma} (\mathbf{n} \times \mathbf{H}_b) \cdot \hat{\mathbf{E}} \, d\Gamma. \quad (2.17)$$

which gives a finite element equation for the time variation of the electric field. The magnetic flux density can then be computed directly after the fact from Faraday's law. There are three different types of boundaries and associated boundary conditions of interest associated with the above formulation:

- Type D: Dirichlet condition on  $\phi$  and a Dirichlet condition for  $\mathbf{n} \times \mathbf{E}$ .
- Type N: A Neumann condition associated with  $\phi$ , e.g.  $\sigma \nabla \phi \cdot \mathbf{n} = 0$ , and a Neumann condition associated with  $\mathbf{H}$ , e.g.  $\mathbf{n} \times \mathbf{H} = 0$ .
- Type P: A Neumann condition for  $\phi$ , e.g.  $\sigma \nabla \phi \cdot \mathbf{n} = 0$  and a Dirichlet condition for  $\mathbf{n} \times \mathbf{E}$ .

Nodal elements are an appropriate basis for  $\phi$  and edge elements are an appropriate basis for  $\mathbf{E}$  to provide tangential continuity. We have included the scalar potential for completeness in the description of the formulation. We will describe results in the next section verifying the formulation for the case with no additional scalar potential.

### 3 Verification Experiments

We consider two verification problems for our quasi-steady method, and compare those solutions to both the analytic solution as well as a comparable problem solved using ALEGRA-MHD. For magnetic field variables, both the quasi-steady state method and ALEGRA-MHD should be second-order accurate in space for problems with smooth velocity fields and orthogonal meshes. For problems with discontinuous velocities or distorted elements, we expect at best first-order accuracy in space. For all of the subsequent discussion, the  $h$  value of the coarsest mesh shown is assigned the value of 1. All finer meshes are assigned values of  $h$  with respect to their refinement from the coarsest mesh.

### 3.1 Solberg-White MHD Shear Problem

We first consider an version of the steady-state Solberg-White problem [5]. The computational domain is a  $[0, 1]$  interval in the  $x$ -direction and periodic in  $y$  and  $z$ . We then apply an initial uniform magnetic field in the  $x$ -direction and an imposed shear velocity in the  $y$ -direction. This motion shears the  $\mathbf{B}$  field and induces a  $y$ -directional component. We use a hyperbolic tangent velocity profile of the form,

$$\mathbf{v}_y(x) = \frac{1}{2} (1 + \tanh(x - 0.5)). \quad (3.18)$$

This produces a nearly linear shear velocity profile that varies smoothly between approximately .26 and .73. Material parameters are chosen such that  $\sigma = \mu = 1$ . This gives us the analytic solution,

$$\mathbf{B}_y = \frac{1}{2} \left( \ln \cosh \frac{1}{2} - \ln \cosh [(x - x_0)] \right). \quad (3.19)$$

We then consider the value of  $\mathbf{B}_y$  for order verification. We do so by uniformly refining the mesh and running both the quasi-steady method (qsm) as well as standard ALEGRA-MHD (mhd). Figure 1 shows the absolute error in the  $y$ -component of the  $\mathbf{B}$  field with respect to mesh refinement. We can clearly see second-order accuracy in space in all

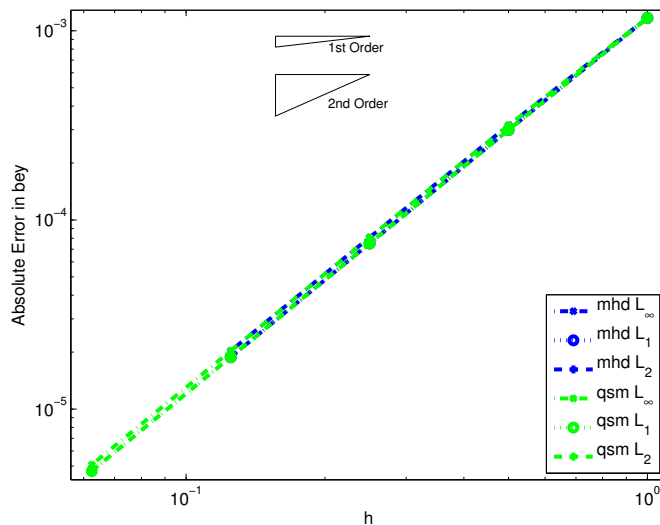


Figure 1: Order verification study indicating second order convergence in the  $y$ -component of the  $\mathbf{B}$  field in the  $L_1$ ,  $L_2$  and  $L_\infty$  norms for both ALEGRA-MHD (mhd) and the Quasi-Steady State Method (qsm) for the MHD shear test problem with a smooth velocity profile.

three norms for both methods. We also note that both the quasi-steady state method

and ALEGRA-MHD produce answers of similar quality. The same data is given in table form in Appendix A.1.

We also consider the solution time for both the quasi-steady state method and ALEGRA-MHD. In both cases we run in serial on `icebox`, which has 3.33 GHz Xeon processors. For ALEGRA-MHD we use the CG solver, while the non-symmetric quasi-steady method uses GMRES. In both cases we precondition using the eddy current preconditioner described in [1] using two Chebyshev smoothing sweeps on each level. The CPU times (in seconds) for this study are shown in Table 1. We note that the quasi-steady method is significantly faster than ALEGRA-MHD, due to the ability to take arbitrarily large timesteps in the fully implicit method. In this case 0.1 seconds of simulation time are covered per timestep. The explicit hydro timestep in ALEGRA-MHD is about 6.25e-4 for the *smallest* problem in the set and the timestep only grows smaller with mesh refinement. Note that this time step could be tuned by adjusting the thermodynamic sound speed in the MHD modeling so these timing numbers should be taken to be primarily illustrative in purpose.

$h$	Solution Time (s)	
	ALEGRA-MHD	Quasi-Steady
1.0	416	2
0.5	692	4
0.25	2,807	16
0.125	19,286	124
0.0625	*	1,377

Table 1: Solution time for the Solberg-White MHD shear problem for the Quasi-Steady State Method (qsm) for the MHD shear test problem with a smooth velocity profile. Asterisks(\*) indicate runs that were prohibitively expensive to complete.

### 3.2 Perry-Jones-White Rotating Cylinder Problem

Our second verification problem is based on White’s version of the Perry-Jones rotor problem [4, 6]. This problem consists of a rotating cylinder in free space with imposed velocity,

$$v_x(r, \theta) = -r\Omega \sin(\theta), \tag{3.20}$$

$$v_y(r, \theta) = r\Omega \cos(\theta), \tag{3.21}$$

where  $\Omega = 10^6$ ,  $(r, \theta)$  are radial coordinates and  $r$  is taken to be 6.554e-3. An initial uniform magnetic field is applied and boundary conditions are imposed matching the

analytic  $\mathbf{B}$  field on the boundaries. The cylinder is then allowed to rotate until the  $\mathbf{B}$  field reaches steady state. Material parameters are chosen with  $\sigma = 4.6575e5$  and  $\mu$  equal to the permeability of free space. Figure 2 shows the steady state distribution of the  $x$  and  $y$  components of the magnetic field in the cylinder and in a surrounding void region.

Figures 3 and 4 show the  $x$  and  $y$  components of the  $\mathbf{B}$  field respectively for both the quasi-steady method and standard ALEGRA-MHD with respect to mesh refinement. We can see first order (or slightly better) convergence in all three norms for both methods. We also note that both the quasi-steady state method and ALEGRA-MHD produce answers of similar quality. It is not clear at this time if the the discontinuity in the velocity field and/or the distorted element shapes are the root cause of the first order convergence rates (rather than second order) in this problem. The same data is given in table form in Appendix A.2.

We again consider the solution time for both the quasi-steady state method and ALEGRA-MHD. We use the machine, preconditioner and solver as in Section 3.1, except that we now use four Chebyshev smoothing sweeps on the fine level and six on intermediate levels of our AMG method. The CPU times (in seconds) for this study are shown in Table 2. We note again that the quasi-steady method is significantly faster than ALEGRA-MHD, due to the ability to take arbitrarily large timesteps in the fully implicit method. In this case  $2e-4$  seconds of simulation time are covered per timestep. The explicit hydro timestep in ALEGRA-MHD is about  $3e-8$  for the *smallest* problem in the set and the timestep only grows smaller with mesh refinement. Again, this time step could be tuned by adjusting the thermodynamic sound speed in the MHD modeling, so these timing numbers should be taken to be primarily illustrative in purpose.

$h$	Solution Time (s)	
	ALEGRA-MHD	Quasi-Steady
1.0	6,318	2
0.5	45,154	7
0.25	*	34
0.125	*	226
0.0625	*	7,461

Table 2: Solution time for the Perry-Jones-White rotating cylinder for the Quasi-Steady State Method (qsm) for the MHD shear test problem with a smooth velocity profile. Asterisks(\*) indicate runs that were prohibitively expensive to complete.

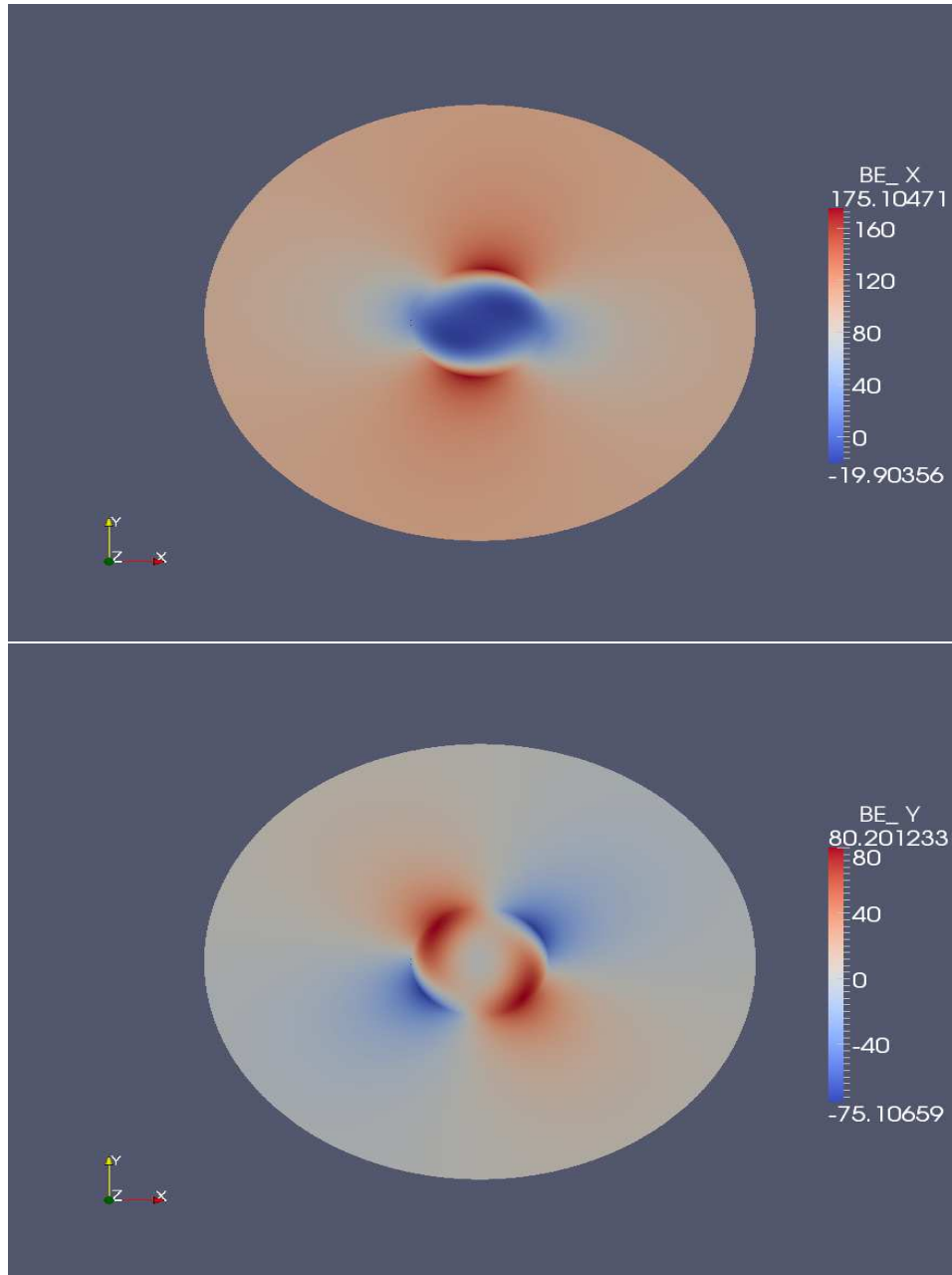


Figure 2:  $x$  and  $y$  components of the steady-state  $\mathbf{B}$  field for the Perry-Jones-White rotating cylinder problem.

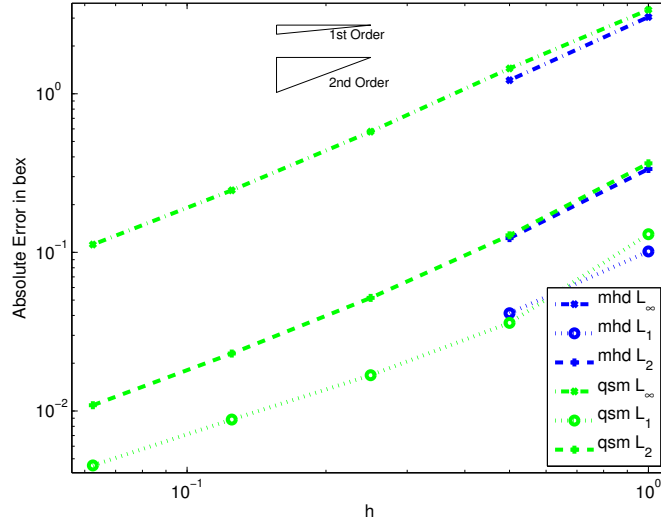


Figure 3: Order verification study indicating first order convergence in the  $x$ -component of the  $\mathbf{B}$  field in the  $L_1$ ,  $L_2$  and  $L_\infty$  norms for both ALEGRA-MHD (mhd) and the Quasi-Steady State Method (qsm) for the Perry-Jones-White rotating cylinder problem.

## 4 Conclusions

We have described our proposed fully implicit formulation for solving 3D quasi-steady state magnetic advection-diffusion problems in an Eulerian frame with a fixed, user-prescribed velocity field. The correctness of implementation was verified on two problems, the Solberg-White magnetic shear problem and the Perry-Jones-White rotating cylinder problem. We have also demonstrated that this quasi-steady state method yield an accurate solution substantially faster than ALEGRA-MHD for problems to which it is applicable.

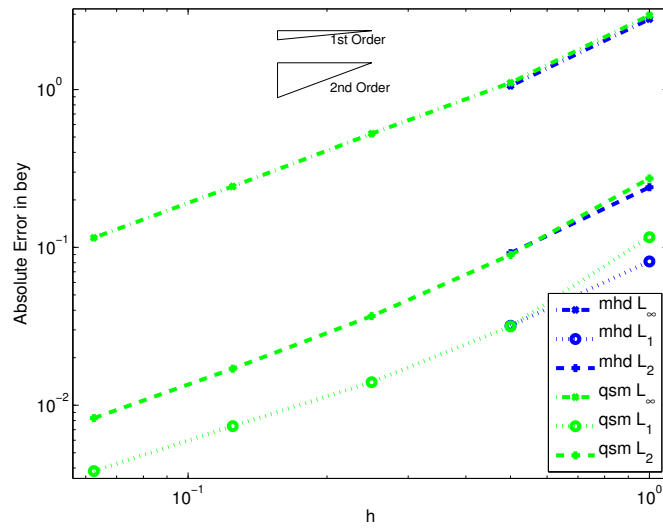


Figure 4: Order verification study indicating first order convergence in the  $y$ -component of the  $\mathbf{B}$  field in the  $L_1$ ,  $L_2$  and  $L_\infty$  norms for both ALEGRA-MHD (mhd) and the Quasi-Steady State Method (qsm) for the Perry-Jones-White rotating cylinder problem.

## References

- [1] P.B. Bochev, J.J. Hu, C.M. Siefert, and R.S. Tuminaro. An algebraic multigrid approach based on compatible gauge reformulations of Maxwell's equations. *SIAM J. Sci. Comput.*, 31(1):557–583, 2008.
- [2] P.B. Bochev and J.M. Hyman. Principles of mimetic discretizations of differential operators. In D.N. Arnold, P.B. Bochev, R.B. Lehoucq, R.A. Nicolaides, and M. Shashkov, editors, *Compatible Spatial Discretizations*. Springer-Verlag, 2006.
- [3] A. Bossavit. Whitney forms: A class of finite elements for three dimensional computations in electromagnetism. *IEEE Proceedings*, 135(8):493–500, 1988.
- [4] M.P. Perry and T.B. Jones. Eddy current induction in a solid conducting cylinder with a transverse magnetic field. *IEEE Transactions on Magnetics*, MAG-14(4):227–232, 1978.
- [5] J. Solberg and D. White. Investigation of the convergence of a MHD shear layer to the jump condition: revised and expanded version 3. Technical report, Lawrence Livermore National Laboratory, November 2008.
- [6] Daniel White. Eddy currents in a rotating cylinder: a code verification problem. Technical report, Lawrence Livermore National Laboratory (unpublished), July 2008.

## A Detailed Verification Results

### A.1 Solberg-White MHD Shear Problem

$h$	Convergence Norm		
	$L_\infty$	$L_1$	$L_2$
1.0	1.16907e-03	1.16907e-03	1.16907e-03
0.5	3.16364e-04	2.98813e-04	2.99328e-04
0.25	8.07924e-05	7.50884e-05	7.52596e-05
0.125	2.03086e-05	1.87955e-05	1.88411e-05

Table 3: Order verification study indicating second order convergence in the  $y$ -component of the  $\mathbf{B}$  field in the  $L_1$ ,  $L_2$  and  $L_\infty$  norms for ALEGRA-MHD (mhd) for the MHD shear test problem with a smooth velocity profile. This is the table form of the MHD data shown in Figure 1.

$h$	Convergence Norm		
	$L_\infty$	$L_1$	$L_2$
1.0	1.16907e-03	1.16907e-03	1.16907e-03
0.5	3.16364e-04	2.98813e-04	2.99328e-04
0.25	8.07924e-05	7.50884e-05	7.52596e-05
0.125	2.03086e-05	1.87955e-05	1.88411e-05
0.0625	5.08477e-06	4.70067e-06	4.71225e-06

Table 4: Order verification study indicating second order convergence in the  $y$ -component of the  $\mathbf{B}$  field in the  $L_1$ ,  $L_2$  and  $L_\infty$  norms for the Quasi-Steady State Method (qsm) for the MHD shear test problem with a smooth velocity profile. This is the table form of the QSM data shown in Figure 1.

### A.2 Perry-Jones-White Rotating Cylinder Problem

$h$	Convergence Norm		
	$L_\infty$	$L_1$	$L_2$
1.0	3.38531e+00	1.30128e-01	3.64433e-01
0.5	1.44313e+00	3.59122e-02	1.28131e-01
0.25	5.76555e-01	1.68215e-02	5.16299e-02
0.125	2.46104e-01	8.82628e-03	2.30312e-02
0.0625	1.12036e-01	4.53553e-03	1.08674e-02

Table 5: Order verification study indicating first order convergence in the  $x$ -component of the  $\mathbf{B}$  field in the  $L_1$ ,  $L_2$  and  $L_\infty$  norms for the Quasi-Steady State Method (qsm) for the Perry-Jones-White rotating cylinder problem. This is the table form of the QSM data shown in Figure 3.

$h$	Convergence Norm		
	$L_\infty$	$L_1$	$L_2$
1.0	2.95058e+00	1.16006e-01	2.73357e-01
0.5	1.10440e+00	3.16109e-02	8.96377e-02
0.25	5.25072e-01	1.39884e-02	3.66707e-02
0.125	2.43420e-01	7.37389e-03	1.70423e-02
0.0625	1.15077e-01	3.82108e-03	8.28454e-03

Table 6: Order verification study indicating first order convergence in the  $y$ -component of the  $\mathbf{B}$  field in the  $L_1$ ,  $L_2$  and  $L_\infty$  norms for the Quasi-Steady State Method (qsm) for the Perry-Jones-White rotating cylinder problem. This is the table form of the QSM data shown in Figure 4.

## DISTRIBUTION:

1 MS 0378  
Allen C. Robinson, 1431

1 MS 0378  
Christopher M. Siefert, 1431

1 MS 0378  
Randall M. Summers, 1431

1 MS 1189  
Christopher J. Garasi, 1641

1 MS 1320  
Pavel B. Bochev, 1416

2 MS 0612  
Review & Approval Desk,  
For DOE/OST I, 9612

1 MS 0899  
Technical Library,  
9536 (electronic copy)